AIP | Journal of Applied Physics

Acousto-optic interaction in photonic crystals with defects

Xiao-Shi Qian, Jing-Ping Li, Ming-hui Lu, Yan-qing Lu, and Yan-feng Chen

Citation: J. Appl. Phys. **106**, 043107 (2009); doi: 10.1063/1.3204018
View online: http://dx.doi.org/10.1063/1.3204018
View Table of Contents: http://jap.aip.org/resource/1/JAPIAU/v106/i4
Published by the American Institute of Physics.

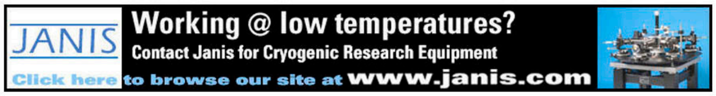

JOURNAL OF APPLIED PHYSICS **106**, 043107 (2009)

Acousto-optic interaction in photonic crystals with defects

Xiao-Shi Qian, Jing-Ping Li, Ming-hui Lu, Yan-qing Lu,[a] and Yan-feng Chen[a]
Department of Materials Science and Engineering and National Laboratory of Solid State Microstructures, Nanjing University, Nanjing 210093, People's Republic of China

(Received 29 March 2009; accepted 12 July 2009; published online 26 August 2009)

The acousto-optic (AO) effects of photonic crystals (PCs) were studied. Both the PCs' periodicity and their index distribution could be modulated instantly by the propagating acoustic wave. As a consequence, the PCs' band structure becomes tunable. In addition to band gap shift in an ideal PC, AO frequency modulation was observed in a PC with single defect, which is quite different from normal AO tunable filters and gives rise to some interesting applications. Furthermore, in dual-defect situation, synchronized and desynchronized modulations were realized at different acoustic wavelengths. Interesting phenomena such as dual frequency sweeping and dual frequency Q-switching were demonstrated. © *2009 American Institute of Physics*. [DOI: 10.1063/1.3204018]

I. INTRODUCTION

Since the concept of photonic crystals (PCs) was proposed by Yablonovich and John in 1987,[1,2] the propagation of electromagnetic (EM) waves in dielectric microstructures has drawn many attentions. Due to the periodic dielectric constant induced photonic band gaps (PBGs), PCs have shown attractive applications in signal processing, optical communications, and even photovoltaic panels.[3–6] However, if the periodicity is broken by inducing a defect into a PC, localized defect modes may appear inside the band gap, which is the fundamental of PC based waveguides and microcavities. In the simplest one-dimensional (1D) case, both high-Q factor defect mode filters and flat-top band-pass filter have been demonstrated.[7,8] If some active media are introduced, laser emission could be realized at the defect mode. Even dual or multichannel filtering or laser emission could be achieved as long as suitable structural parameters are designed.[9]

However, the characteristics of a PC are normally fixed once its structure is settled, while people pursue tunability for agile photonic devices. Therefore a lot of efforts have been made toward reconfigurable PCs. In 1999, Busch and John[10] reported a tunable PC defect mode using liquid crystal (LC) as a filler; Du *et al.*[11] reported an electrically tuned photonics crystal fiber also with LC filling. However, inducing extra materials into PCs is not convenient. The LC alignment inside a PC is hard to control. In addition, the response time of a LC device is typically in millisecond level, which might be too slow for some applications.[12] Although electro-optic (EO) tuning is also applicable to a PC, the index change in EO crystals is small and the driving voltage is normally high to kilovolt level.[13] It is quite desirable to develop simple and low voltage tuning techniques for various PCs. Not only the band gap, but also the defect mode's position, intensity and Q factor are expected to be controlled freely. We believe this is very important toward the real applications of PCs, especially for the PC based lasers.

Acousto-optic (AO) effect has been widely used to process light signals for years. Both light intensity and polarization could be manipulated through AO effects.[14] There is even observation of angular momentum transfer between photons and phonons through AO interaction.[15] However, the AO effect is normally studied and realized in homogeneous materials such as optical glasses and crystals. AO interactions in inhomogeneous materials still have not drawn many attentions.[16–18] It is interesting to see how the acoustic wave affects artificial microstructures such as PC defects. From another point of view, the electron-phonon interaction plays an important role in electrons' state transition in a crystal,[19] one would also expect interesting and useful physical effects in a PC with acoustic wave propagation. Both some fundamental properties and promising applications are foreseeable.

In this paper, we studied the AO interaction in photonic crystals with defects. We found that the PCs' defected mode is very sensitive to the induced longitudinal acoustic waves. PCs with both single defect and dual defects were investigated. Some interesting phenomena such as frequency tuning and AO dual frequency Q-switching were demonstrated, which should be useful for PC based lasers.

II. MODEL AND SIMULATION APPROACH

As we know, a perfect 1D PC is formed by a series of periodic units that may be described as $(AB)^n$, where A and B stand for different layers with different refractive indices. n means the total layer number of the PC. When light propagates in a PC, the index mismatch results in periodic partial reflections at A/B boundaries. They could be viewed as a serial of secondary "sources." In a certain wavelength, all periodic secondary sources may interfere constructively at the backward direction, which corresponds to a PBG and causes a strong light reflection. However, acoustic wave induces both variable strain and index change, the original PC's structural periodicity thus is broken. The "interference" of all reflected beams at A/B boundaries changes consequently. Band structure change is expected.

To model the AO effects in a 1D PC, we assume a longitudinal wave traveling along z axis, which is normal to

---

[a] Authors to whom correspondence should be addressed. Electronic addresses: yqlu@nju.edu.cn and yfchen@nju.edu.cn.

layer boundaries. The acoustic wave generates deformation that is represented by the displacement value U as

$$U(z,t) = A\cos(\Omega_S t + k_S z), \tag{1}$$

where A is the maximum displacement amplitude; Ω_s and k_s are the angular frequency and the wave vector of acoustic wave, respectively. On the other hand, the acoustic wave induces strain could also be obtained from Eq. (1) as

$$S(z,t) = k_s \bullet A\sin(\Omega_s t + k_s z), \tag{2}$$

where S is the differential of U. According to Eqs. (1) and (2), we may deduce the thickness change ΔU of all A and B layers easily. Obviously these thickness changes vary from time to time along with the acoustic wave propagation. Some parts of units are shrunk while other parts may expand due to acoustic wave at a certain moment, which would induce some interesting effects.

In addition to thickness change ΔU, the PC structure is perturbed by acoustic wave in another way, the refractive indices in both A and B layers also change due to the traditional elasto-optic effect,

$$\Delta n = -\frac{1}{2} n_z^3 p_{11} S(z,t), \tag{3}$$

here n_z and p_{11} represent the original refractive index and the elasto-optic coefficient, respectively.

With deformation ΔU and index change Δn, considering a traveling acoustic wave, we can reconstruct a 1D PC structure based on the index distribution at any certain moment. The time resolved band structure and transmission properties thus could be computed for an acoustic wave modulated PC.

Numerous approaches have been proposed to study PC's optical properties, for example, the transfer matrix method (TMM), plane wave expansion method, multiple scattering theory, and finite-difference time-domain method.[20–23] Among them, TMM is still one of the most effective and simplest ways investigating the properties of EM wave propagating in 1D finite optical structures.

In our model, we consider the EM wave vector is perpendicular to A/B layer boundaries, so that the light's polarization state could be ignored in the simulation. Therefore, according to the TMM,

$$M = \prod_{j=1}^{k} \begin{pmatrix} \cos\delta_j & \dfrac{i}{\eta_j}\sin\delta_j \\ i\eta_j \sin\delta_j & \cos\delta_j \end{pmatrix} = \prod_{j=1}^{k} M_j = \begin{pmatrix} m_{11} & m_{12} \\ m_{21} & m_{22} \end{pmatrix}, \tag{4}$$

$$t = \frac{2\cdot\eta_0}{\eta_0 m_{11} + m_{21} + \eta_0\eta_{k+1} m_{12} + \eta_{k+1} m_{22}}, \tag{5}$$

where t, η_0, η_{k+1} is transmission coefficient, effective refractive index in layer k and layer $k+1$, respectively. The measurable light transmittance is the modular square of complex transmission coefficient t, i.e., $T = \eta_{k+1}/\eta_0 tt^*$. As long as we know the PC's structures and the acoustic wave's features, its transmission properties could be obtained.

To study the AO effects in a PC, the simplest case is an ideal PC structure, meaning no defects, just like an electron's indirect transition when it absorb or emit a photon. There is also a counterpart for photons in a PC. A photon may absorb or emit a phonon then further reflected by the periodic dielectric structure. Because a phonon involves in the photon's interference, a side band thus could come out besides the band gap. However, ideal PCs normally have unsatisfied filtering and lasering characteristics,[24] we would focus our AO effect study on PCs with various defects.

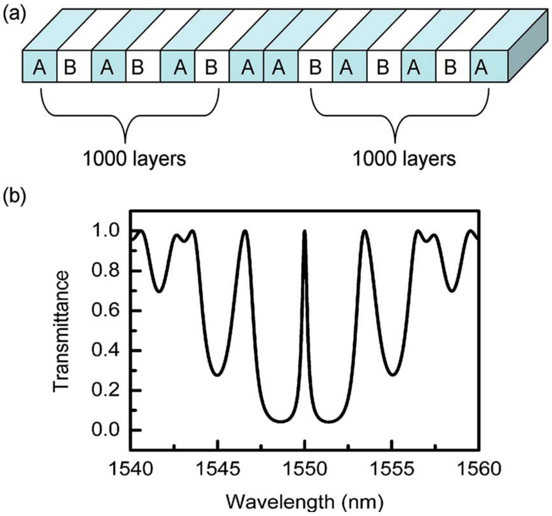

FIG. 1. (Color online) (a) A photon crystal with a single defect at its central area. 1000-layer perfect PC structure locates at each side of the defect for Bragg reflection. ($n_A = 1.46$, $n_B = 1.465$, $d_A = 265.4$ nm, $d_B = 264.5$ nm) (b) TMM simulation showing a single sharp defect mode with 100% transmittance at the middle of the reflection band gap.

III. SIMULATION RESULTS

A. PC with single defect

Based on a perfect PC whose structure is described with $(AB)^n$, we may change its parameters to introduce a single defect, e.g., doubling one layer's thickness to give $\sim\lambda/4$ further light path. Normally this layer is set at the central area of a PC, so a PC with a single defect can be represented by $(AB)^n\, AA(BA)^n$ as shown in Fig. 1(a). Define the indices and thicknesses in A and B layers with n_A, d_A, n_B, and d_B, respectively. Assume $n_A d_A = n_B d_B$, which means all A and B layers have the same light path, so that light in the defect could be forced to resonate in a cavity with two perfect Bragg mirrors. This design guarantees a nice defect transmission mode that happens to appear in the middle of the PBG.

It is well known that the hydrogen loaded SiO_2 has an improved photosensitivity. Its refractive index changes at an order of 10^{-3} after UV exposure.[25,26] A PC structure thus could be achieved through the standard interference or mask approaches. However, the PC structure after UV exposure is still treated as a uniform acoustic medium. Figure 1 illustrates structure and transmission properties of a 1000-period PC with single defect. In our simulation, we set $n_A = 1.46$, $n_B = 1.465$, which correspond to the indices of unexposed and UV-exposed hydrogen-loaded SiO_2, respectively, $d_A = 265.4$ nm, $d_B = 264.5$ nm, which indicate the different layer thicknesses, so that $n_A d_A = n_B d_B = 1550$ nm$/4$. From the figure, the band gap is around 1550 nm with ~ 10 nm band-

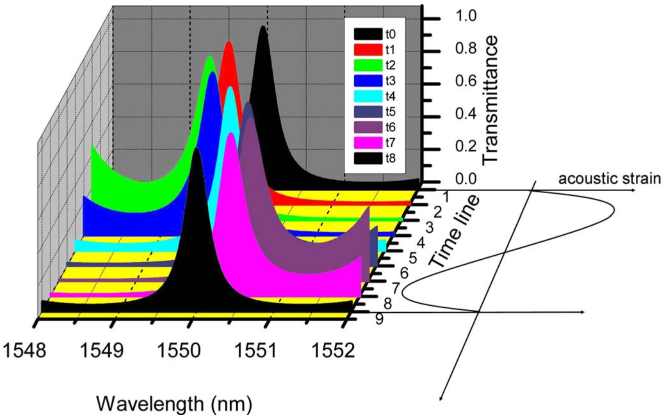

FIG. 2. (Color online) Acoustic wave induced center frequency swing at different moments of the single defect mode showing in Fig. 1. The maximum frequency shift is dominated by acoustic wave intensity.

width. A defect induced transmission peak locates exactly at the band gap center. The corresponding Q-factor is 4300. To adjust the gap's bandwidth or increase the defect mode's Q-factor, more units or larger index fluctuation should be adopted.

Once we consider the propagation of a longitudinal acoustic wave in the PC structure, the transmission properties could be obtained through TMM at any moment. Assume the acoustic wave coupled in the PC in Fig. 1, the maximum induced displacement is 50 nm, for 265 μm acoustic wavelength, corresponding strain at 10^{-4} level, which is achievable. The acoustic wave frequency is ~21 MHz for the acoustic velocity in fused silica, which is 5600 m/s. This case is very practical as its counterpart in crystals is the interaction between electrons and long-wave acoustic branch photons near a defect. From Fig. 2, the optical transmission property of this PC is obtained. The defect mode has periodic swing from its original wavelength. The swing speed is determined by acoustic wave's frequency. Faster modulation can be obtained with higher frequency. The origin of the defect mode modulation is not complicated. The acoustic wave induced periodic index and thickness change of the defect layer AA. As a result, light path of central defect changes with the acoustic wave, the corresponding defect mode wavelength changes consequently. As long as the acoustic wave does not affect the PC periodicity too much, the PC may still maintain enough Bragg reflection to support the defect mode. Other features do not change evidently including the defect mode's transmittance and Q-factor. Since a long acoustic wave is considered in our study, this assumption is normally valid. From Fig. 2, the spectral shape of the defect mode does not show much difference.

As we know, AO tunable filter (AOTF) has been widely used for many applications. The center transmission wavelength of an AOTF is determined by acoustic frequency. However, although the AO interaction in a PC with defect also shows tunable transmission, it has a different mechanism. The acoustic wave's intensity dominates the transmission frequency, which might be useful in sensor applications. If there is a narrow band incidence light source, a pulsed light output around the defect mode will be observed. When a wide band source is employed, a periodic wavelength variable source may be obtained. If introducing active medium in a PC,[27] a frequency modulated laser could be realized.

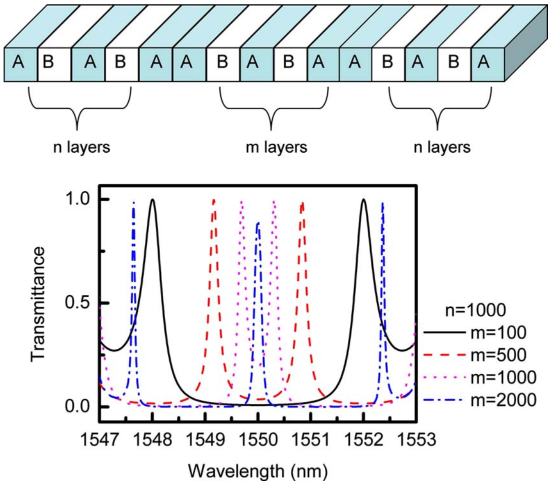

FIG. 3. (Color online) Transmission spectra of dual-defect photonic crystals with a changing m factor are shown. $n=1000$. m and n represent the number of layers between the two defects and the number of layers outside the defects, respectively.

B. PC with dual defects

In addition to single defect, more defects also could be induced to a PC, which might have more interesting properties. We define PCs with dual defects be described with $(AB)^nAA(BA)^mA(BA)^n$. Set $n_Ad_A=n_Bd_B=1550$ nm/4 to obtain band gap at 1550 nm telecom window. Here m factor determines the distance between two defects. When these two defects are well separated, e.g., $m\geq 2n$, the two defect modes will not influence transmission so they could be viewed as two independent PCs with single defect. The dash-dot curve in Fig. 3 shows the result, where $m=2n=2000$. Only a degenerated defect mode was found but its transmittance is a little lower than that of the single defect case. However, if the distance between two defects becomes closer, e.g., $m<2n$, interaction between these two defects become stronger thus the defect mode is split to two peaks. The peak separation becomes farther as the two defects getting closer and closer as shown in Fig. 3. Just like the single defect case, we also studied the AO interaction in PCs with dual defects, but they are categorized to two kinds: synchronized AO modulation and desynchronized AO modulation.

Here synchronized modulation indicates when the distance between two defects are equal to the integral multiples of the wavelength of the propagating acoustic wave. Accordingly the two defects in PCs will be stressed or pulled in the same way during acoustic wave propagation so that the light path of two defects will always be the same. On the contrary, desynchronized modulation represents other situations as long as the distance between two defects does not equal to the integral multiples of the acoustic wavelength.

Just like the case of single defect, the frequency swing of defect modes' transmission peaks is also observed as the two defects always have the same deformation. In our simulation, in order to satisfy the synchronized modulation, we set the

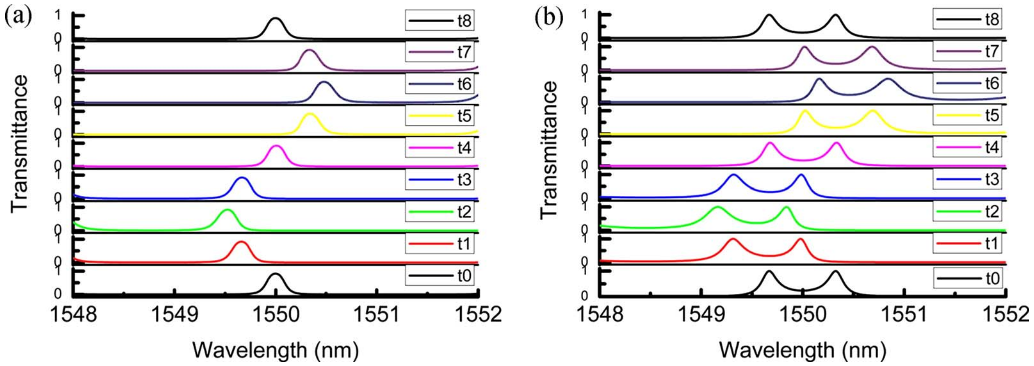

FIG. 4. (Color online) Time resolved synchronized modulation of dual-defect modes. $t0$-$t8$ means different moments. (a) Uncoupled situation with an $(AB)^nAA(BA)^mA(BA)^n$ type structure, $m=2000$, $n=1000$, the acoustic wavelength is 265 μm. (b) Coupled situation with an $(AB)^nAA(BA)^mA(BA)^n$ type structure, $m=1000$, $n=1000$, the acoustic wavelength is 265 μm. m,n represent the number of layers of such part of structure.

acoustic wavelength as the length of 1000 layers. We obtained single [Fig. 4(a)] and dual frequency sweeping [Fig. 4(b)] in uncoupled and coupled dual defect modes, respectively. 0.9 nm tuning range was achieved giving a 50 nm acoustic wave displacement amplitude. The dual-frequency modulation might have some unique applications in filtering and signal processing.

Unlike the straightforward synchronized modulation, the desynchronized modulation is more complicated and interesting. Just detune the acoustic wavelength so that the distance between two defects is not the multiples of acoustic wavelength. In this situation, two defects deform in different ways and cause different phase delays. One defect may expand but another one may shrink. The corresponding defect modes thus are modulated in different ways, which are reflected in the PC's transmission curves. However, no matter what distance between the two defects, there are at least two certain moments that the two defects have the same deformation in an acoustic wave period. The two defect modes thus have the same transmission peak; a light pulse is able to pass through. However, at an arbitrary time, the defects are modulated in different ways for light may not pass though two defects simultaneously. The AO PC filter is then shut off. Figure 5 shows our simulation results. The defect distances are 2.5 and 2.25 times of acoustic wavelength in Figs. 5(a) and 5(b), respectively. The acoustic wavelength is 265 μm corresponding to the acoustic frequency of 21 MHz in fused silica. In Fig. 5(a), the acoustic wave's phases are always opposite because of the half-wave distance. If one defect is expanding, another one is shrinking. Only at the time both defects have no deformation, their transmission peaks are overlaid. A periodic pulsed transmission thus is obtained but the frequency in time domain is doubled. A 21 MHz acoustic wave may generate frequency doubled 42 MHz pulsed light transmission. In another point of view, the Q-factor of the defect mode, which is modulated by the acoustic wave changes from 12 900 to 0 periodically. This might be an AO Q-switching approach that could be used for PC based active

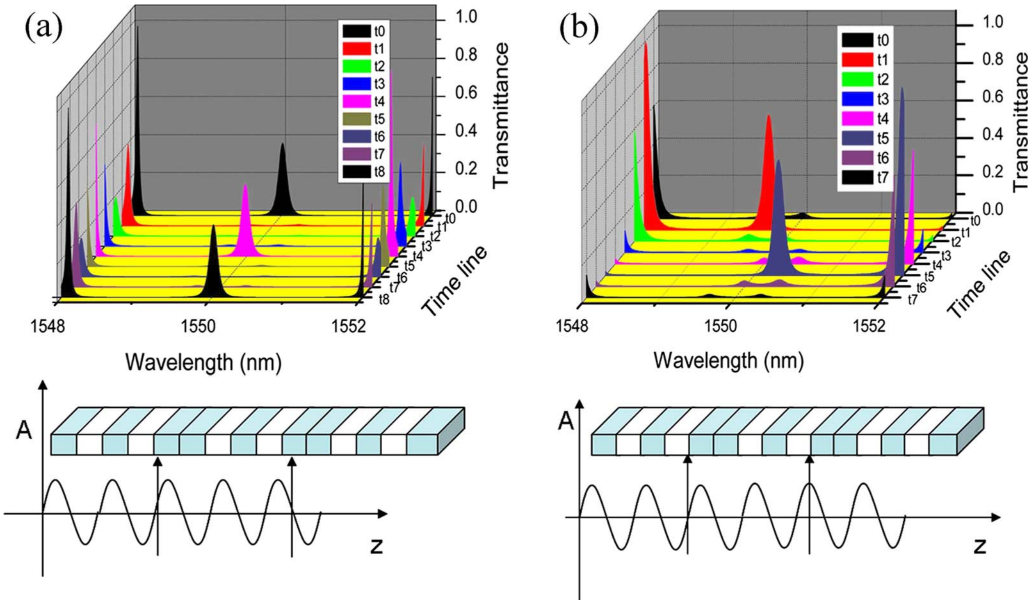

FIG. 5. (Color online) Time resolved desynchronized modulation of dual-defect modes. $t0$-$t8$ means different moments in one acoustic period. (a) $(AB)^nAA(BA)^mA(BA)^n$ type structure, $m=2500$, $n=1000$, the acoustic wavelength is 265 μm. The space between two defects is 2.5 times of acoustic wavelength. (b) $(AB)^nAA(BA)^mA(BA)^n$ type structure, $m=2250$, $n=1000$, the acoustic wavelength is 265 μm. The space between two defects is 2.25 times of acoustic wavelength. m,n represent the number of layers of such part of structure.

components. On the other hand, when the distance between these two defects decreases as shown in Fig. 5(b), the defects are either expanded or shrunk when they have the same deformation. As a consequence, pulsed transmission emerges at two wavelengths successively. Adjusting the acoustic wave's intensity may further change the wavelengths of the transmitted pulses. A tunable dual wavelength AO Q-switching thus is achieved. If the distance between two defects becomes closer, the similar results of Q-factor modulation still exist in the coupled dual-defect situation as long as the distance satisfied $0.5+a$, $0.25+a$ times of acoustic wavelength, $a=0,1$. When the two defects are much closer than 0.25 times of acoustic wavelength, the acoustic modulation to two defects are almost the same. In the case, it is more like a synchronized modulation, as represented by Fig. 4(b), rather than the desynchronized situation. However, the distance between two transmission peaks is even wider due to stronger defect mode coupling.

IV. CONCLUSIONS

Both AO effects and 1D PC have been research topics for years. However, our study shows that the combination of these two classical subjects still contains interesting physics and useful applications. In this work, we studied the AO interaction in photonic crystals with defects. Some encouraging results are demonstrated. Because the acoustic wave may affect PCs' periodicity and redistribute the refractive indices, the PCs' transmission properties thus are modulated. Unlike the traditional AO effect in homogeneous materials, defect model frequency sweeping was observed in a PC with single defect. In dual-defect situation, synchronized and desynchronized modulations were realized at different acoustic wavelengths. Interesting phenomena such as dual-frequency sweeping and Q-switching were revealed. Since defect mode plays an important role in many PC based applications,[7–9,27,28] our approach may supply a unique way to manipulate those processes though AO effect. As our setup is sensitive to the sound's intensity and frequency, a sound detection and characterization technique may be developed as well.

ACKNOWLEDGMENTS

This work was sponsored by NSFC Program under Contract No. 10874080, the Nature Science Foundation of Jiangsu Province under Contract No. BK2007712 and Quantum Manipulation Program under Contract No. 2006CB921805. Yan-qing Lu acknowledges the support from China MOE for new century and Changjiang scholars program.

[1] E. Yablonovitch, Phys. Rev. Lett. **58**, 2059 (1987).
[2] S. John, Phys. Rev. Lett. **58**, 2486 (1987).
[3] S. Y. Lin, J. G. Fleming, and I. El-Kady, Appl. Phys. Lett. **83**, 593 (2003).
[4] M. Scalora, J. P. Dowling, C. M. Bowden, and M. J. Bloemer, J. Appl. Phys. **76**, 2023 (1994).
[5] G. D'Aguanno, E. Angelillo, C. Sibilia, M. Scalora, and M. Bertolotti, J. Opt. Soc. Am. B **17**, 1188 (2000).
[6] M. Scalora, R. J. Flynn, S. B. Reinhardt, and R. L. Fork, Phys. Rev. E **54**, R1078 (1996).
[7] D. S. Wiersma, P. Bartolini, A. Lagendijk, and R. Righini, Nature (London) **390**, 671 (1997).
[8] C. H. Chen and Y. Fainman, IEEE J. Sel. Top. Quantum Electron. **13**, 262 (2007).
[9] Z. Wang and R. W. Peng, Appl. Phys. Lett. **84**, 3969 (2004).
[10] K. Busch and S. John, Phys. Rev. Lett. **83**, 967 (1999).
[11] F. Du, Y. Q. Lu, and S. T. Wu, Appl. Phys. Lett. **85**, 2181 (2004).
[12] Y. Q. Lu, F. Du, Y. H. Lin, and S. T. Wu, Opt. Express **12**, 1221 (2004).
[13] A. Yariv and P. Yeh, *Optical Waves in Crystals* (Wiley, New York, 1983).
[14] H. Gnewuch, N. K. Zayer, and C. N. Pannell, Opt. Lett. **25**, 305 (2000).
[15] P. Z. Dashti, F. Alhassen, and H. P. Lee, Phys. Rev. Lett. **96**, 043604 (2006).
[16] P. St. J. Russell, Phys. Rev. Lett. **56**, 596 (1986).
[17] W. L. Liu, P. St. J. Russell, and L. Dong, Opt. Lett. **22**, 1515 (1997).
[18] S. Krishnamurthy and P. V. Santos, J. Appl. Phys. **96**, 1803 (2004).
[19] J. Bardeen, L. N. Cooper, and J. R. Schrieffer, Phys. Rev. **108**, 1175 (1957).
[20] L. Y. Bahar, J. Engrg. Mech. Div. **98**, 1159 (1972).
[21] K. M. Ho, C. T. Chan, and C. M. Soukoulis, Phys. Rev. Lett. **65**, 3152 (1990).
[22] L. M. Li and Z. Q. Zhang, Phys. Rev. B **58**, 9587 (1998).
[23] K. Yee, IEEE Trans. Antennas Propag. **14**, 302 (1966).
[24] T. F. Krauss, O. Painter, A. Scherer, J. S. Roberts, and R. M. De La Rue, Opt. Eng. **37**, 1143 (1998).
[25] T. Erdogan, V. Mizrahi, P. J. Lemaire, and D. Monroe, J. Appl. Phys. **76**, 73 (1994).
[26] O. Guan, H. Y. Tam, X. M. Tao, and X. Y. Dong, IEEE Photonics Technol. Lett. **12**, 1349 (2000).
[27] M. H. Shih, A. Mock, M. Bagheri, N.-K. Suh, S. Farrell, S.-J. Choi, J. D. O'Brien, and P. D. Dapkus, Opt. Express **15**, 227 (2007).
[28] M. J. Steel, M. Levy, and R. M. Osgood, IEEE Photonics Technol. Lett. **12**, 1171 (2000).